

# 14

## Heavy quarks

### 14.1 Introduction

When quarks were introduced into physics, they were considered to be light, like the up, the down, and the strange quarks. Their bound states were light mesons, such as the  $\pi$  and K mesons. In fact, light states were interpreted as the Goldstone bosons of the SU(3) symmetry with several of the aspects of Goldstone particles discussed in Chapter 5.

The next quark is the charm quark, which was formulated in order to suppress flavor-changing-neutral couplings in the K mesons (Glashow *et al.*, 1970) (GIM henceforth). Since the charm quark is much heavier than the proton, its existence gave rise to the possibility that additional heavy quarks may exist. The expectation was confirmed with the discoveries of the bottom and top quarks when accelerators of higher and higher energies began operating.

The precise definition of quark masses is a delicate topic and for this reason we shall discuss some of the issues involved. Masses of fermions appear in the electroweak Lagrangian after the breaking of the symmetry, i.e. when the Higgs field acquires a vacuum expectation value. Masses for particles are measured through their interactions with an external field; for example, the bending of an electron beam in a magnetic field determines the ratio  $e/m$ . The interaction contains higher-order corrections, which must be included. For leptons the masses are defined as poles of the propagators. For quarks the situation is more complicated because they never appear as free particles, but are always confined within hadrons. The masses of quarks must include radiative corrections from the forces which confine them. On the energy scale of the heavy quarks the strong coupling constant is small enough to allow perturbative calculations. We define the running quark mass  $m(p^2)$  as the renormalized mass parameter in the quark propagator

$$S(p) = \frac{i}{\not{p} - m_0 - \Sigma(p) + i\varepsilon} = \frac{iZ_3(p)}{\not{p} - m(p^2) + i\varepsilon}. \quad (14.1)$$

In this expression  $m_0$  is the bare mass and  $\Sigma(p)$  is the fermion self-energy correction obtained in perturbation theory, which contains infinite terms. The infinite terms combine with  $m_0$  to define the physical mass and define the wave-function renormalization  $Z_3(p)$ . The specific method for eliminating (subtracting) the infinity is scheme-dependent and brings into the definition of masses and coupling constants the renormalization scale  $\mu_0$ , where the subtraction takes place. This is very similar to the definition of the running coupling constant described in Section 11.2.

So far have we defined quark masses as functions of the renormalization point  $\mu_0$  and the momentum  $p$  at which they are measured. We need an additional prescription for relating them to masses of hadrons or for describing how we estimate reactions in which heavy quarks occur. There are several methods for extracting quark masses from physical processes. One of them uses sum rules over two-point functions (spectral functions), which are saturated by physical data and are matched to theoretical expressions that include running quark masses (Narison, 2001; Manohar, 2000). Another method appeals to decays of mesons containing a single heavy quark. Here one computes the decay in a two-fold expansion: in powers of  $\alpha_s(p)$  and a non-perturbative series in powers of  $\Lambda_{\text{QCD}}/m_Q$  (Manohar and Wise, 2000). The masses extracted by the various methods are close to each other and contain an explicit dependence on the momentum at which they are measured. The spectrum that emerges for the new quarks is

$$\begin{aligned}m_c(m_c) &= 1.15\text{--}1.35 \text{ GeV}, \\m_b(m_b) &= 4.6\text{--}4.9 \text{ GeV}.\end{aligned}$$

The mass of the top quark is determined in another way. The observed events are attributed to the production of  $t\bar{t}$  pairs and their subsequent decays into leptons and hadron jets. The production of the pairs is computed in the parton model using lowest-order QCD. The value for the top quark appears in the calculation and the value which optimizes the fit is reported as the standard-model mass, giving (CDF/DO, 2005)

$$m_t = 174.3 \pm 3.4 \text{ GeV}.$$

Besides the masses of the heavy quarks we need their couplings to charged and neutral currents. They are accurately determined by the gauge nature of the theory and experimental data. The couplings have already been discussed in Chapter 9.

There are several other properties of heavy quarks that we take up in this chapter. First, the decays of states containing heavy quarks involve hadronic matrix elements that simplify considerably. In addition, when they appear as intermediate states in loop diagrams, they dominate the diagrams and produce new phenomena such as

the mixing of states and CP asymmetries. Examples of the new phenomena are (i)  $B^0-\bar{B}^0$  mixing dominated by box diagrams and (ii) some CP asymmetries dominated by penguin diagrams. Finally, heavy quarks may have strong couplings to induce bound states that imitate the Higgs particles. Some of these topics will be covered in this and the following chapters.

It is still interesting to ask which quarks are considered to be heavy. A heavy state is one with

$$m_q \gg \Lambda_{\text{QCD}},$$

where according to QCD the interparticle forces become weak. For instance, the inclusive semileptonic decays of pseudoscalar mesons containing a heavy quark must be given to a first approximation by the spectator model. The spectator model, improved by the momentum distribution of a b quark in a B meson, gives an accurate description of semileptonic B-meson decays. Thus B and higher meson states are considered to be heavy states. In fact, for hadronic states containing a heavy quark, a systematic expansion has been developed in inverse powers of the heavy-quark mass, which will be described in Sections 14.4 and 14.5. The top quark decays so fast that bound states do not have enough time to form.

A crude test for the validity of the spectator model is provided by the ratio of lifetimes of charged and neutral mesons. For mesons with beauty quarks,

$$\frac{\tau_{B^+}}{\tau_{B^0}} = 1.08 \pm 0.01,$$

which is to be compared with the ratio for mesons containing charmed quarks,

$$\frac{\tau_{D^+}}{\tau_{D^0}} = 2.55 \pm 0.01.$$

The ratio for the B mesons suggests that the spectator model is applicable. The ratio for D mesons indicates that there are additional contributions. In fact, it was a surprise when the experimental colleagues established this large ratio. It is now generally believed that annihilation diagrams are important in D-meson decays. The simple picture that mesons consist of a quark and an antiquark is too naive, because the gluons in D mesons play a very active role in binding the quarks. We illustrate this fact by the following argument, where we set the CKM matrix equal to the unit matrix, which makes the  $V_{cd}$  element zero. The spectator decay mode (see Section 14.2)

$$c \rightarrow s + \bar{d} + u$$

is expected to give equal contributions to  $D^0$  and  $D^+$  decays, and its amplitude will be denoted by  $A_{\text{sp}}$ . In addition, for the  $D^0$  meson there is the annihilation diagram

for the reaction

$$c + \bar{u} \rightarrow s + \bar{d} + \text{gluons},$$

with a  $W^+$  exchanged in the t-channel. Its amplitude will be denoted by  $A_{\text{an}}$ . The decay width for  $D^0$  depends on the sum of the two amplitudes,

$$\Gamma_{D^0} \propto |A_{\text{sp}}|^2 + |A_{\text{an}}|^2,$$

and similarly for  $D^+$ ,

$$\Gamma_{D^+} \propto |A_{\text{sp}}|^2.$$

The CKM-matrix elements are the same in all these diagrams, indicating that the lifetime  $\tau_{D^+}$  is larger than  $\tau_{D^0}$ . Precise calculations for these and other decays of charm mesons are difficult, but there are phenomenological models that give a consistent picture for several decay channels (Bander *et al.*, 1980).

This chapter is long and contains various topics. To help the reader I outline its contents. The following three sections describe decays of heavy quarks in phenomenological models. Some of these models have been very popular. Sections 14.4 and 14.5 are devoted to the heavy-quark effective theory (HQET), which is a systematic expansion of amplitudes in inverse powers of the heavy-quark mass. The top quark is very heavy and has special properties. For this reason a special section is devoted to it. Finally, heavy quarks play an important role in loop diagrams, with a simple example being provided by box diagrams, which are ultraviolet-finite. An introduction to the computational methods for box diagrams is included in Section 14.7.

## 14.2 Semileptonic and inclusive B-meson decays

### 14.2.1 The spectator model

When a heavy quark, generically denoted by  $Q$ , decays inside a hadron, it does so without disturbing the surrounding field produced by other quarks, antiquarks, and gluons. In the B mesons, for instance, the b quark decays, leaving the light antiquark u, d, or s (hereafter generically denoted as q) undisturbed (spectators). Thus we expect the decay of the B meson to be given by the free decay of the b quark to a zeroth-order approximation. This result must be improved for the bound-state effects of the meson, as will be described in this section (Altarelli *et al.*, 1982).

In the spectator model, the light quark moves in the field of the heavy quark, and between them they share all the energy and momentum of the meson. The spectator quark q has a definite mass  $m$  and a four-momentum  $p_q \equiv (E_q, \mathbf{p})$ . In the rest frame of the meson the b quark moves with a virtual mass  $W$  and a

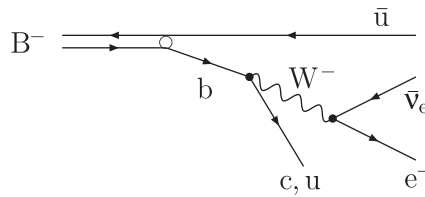


Figure 14.1. B-meson decay.

four-momentum  $p_b \equiv (E_b, -\mathbf{p})$ , where

$$E_q + E_b = M_B, \tag{14.2}$$

$$W^2 = M_B^2 + m_q^2 - 2M_B\sqrt{\mathbf{p}^2 + m_q^2},$$

and  $M_B$  is the mass of the B meson. The decay is now given by the point-like decay of the b quark averaged over its momentum inside the meson (Fig. 14.1).

In the model of Altarelli *et al.* (1982), henceforth called the ACCMM model, the averaging over the momentum of the b quark is done by introducing a Gaussian distribution function,

$$\phi(|\mathbf{p}|) = \frac{4}{\sqrt{\pi} p_F^3} \exp(-|\mathbf{p}|^2/p_F^2), \tag{14.3}$$

where  $p_F$ , the Fermi momentum, is a free parameter to be adjusted by comparing the theoretical prediction with the experimental spectrum. Its value is of the order of a few hundred MeV at most, so large- $\mathbf{p}$  configurations are exponentially suppressed. With this distribution the b quark remains close to its mass shell.

To calculate the electron spectrum from the semileptonic decay  $b \rightarrow u(c)e\bar{\nu}_e$ , one follows three steps.

1. One calculates the differential decay width for a point quark in its rest frame. This is exactly analogous to the muon decay and the result is

$$\frac{d\Gamma^0}{dE} = \frac{G^2 W^4}{48\pi^3} |V_{u(c)b}|^2 x^2 (3 - 2x). \tag{14.4}$$

Here,  $E$  is the electron energy,  $V_{ub}$  or  $V_{cb}$  are the CKM-matrix elements, and  $x = 2E/W$ . Note that we have neglected the masses of all final-state particles, which is surely not justified for a  $b \rightarrow c$  transition, with the relevant mass dependences given in the ACCMM article.

2. In addition, one may incorporate the QCD corrections to this tree-level decay distribution, by multiplying  $d\Gamma^0/dE$  by an overall factor that is less than unity and depends upon  $x$ . This changes the shape of the spectrum near its endpoint. This will not be discussed here, but is described briefly in Problem 2.

3. The decaying quark is not at rest but moves with a momentum  $|\vec{p}|$  inside the meson. We can account for this motion by writing the decay rate in a Lorentz-invariant form, which will be valid in any frame. To this end, we write first

$$x = \frac{2E}{W} = \frac{2p_b \cdot p_e}{W^2} = \frac{2}{W^2}(E_b E_e - p p_e \cos \theta). \quad (14.5)$$

The first two equations are computed in the rest frame of the b quark and the third one in a frame where the b quark moves. Here  $E_b^2 = W^2 + p^2$ ,  $p_e^2 = E_e^2 - m_e^2$ , and  $\theta$  is the angle between the momentum of the b quark and the direction of the electron. The final decay rate is obtained by averaging over  $p$  and  $\theta$  using the distribution function

$$\frac{d\Gamma}{dE_e} = \frac{G^2}{48\pi^3} |V_{ub}|^2 \int_0^{p_F} W^4 x^2 (3 - 2x) \phi(p) p^2 dp d\cos\theta; \quad (14.6)$$

here  $x$  depends on  $p$  and the range of integration over  $\theta$  is from 0 to  $\pi$ .

This method of averaging over the Fermi motion respects Lorentz invariance and takes into account the phase space. It is somewhat crude, in the sense that the energy and momentum of the meson are supposed to be distributed between the two constituent quarks only and the distribution formula is valid only when  $|\mathbf{p}|$  is rather small. In spite of its crudeness, the model describes accurately the electron spectrum observed in the experiments. It indicates that for B and heavier mesons the spectator model is a reasonable zeroth-order approximation, requiring additional corrections from the interaction of the heavy quark with its surrounding field. We shall discuss some improvements in this chapter.

### 14.2.2 The parton model

The semileptonic B-meson decays can be presented by the diagram in Fig. 14.2, where X can be a specific final state or the incoherent sum over various final states. The drawing represents the square of the amplitude and looks very much like the diagram for deep inelastic scattering. This suggests that a formally similar analysis for the B-meson inclusive decays is possible. There are two differences, however; the initial B meson is heavy and the current is time-like, with its variables determined by the initial and final hadronic states. Consequently, we use the same formalism but the structure function is now different, giving the probability of finding a b quark in a fast-moving B meson.

In a standard analysis the square of the matrix element is given as the product of a leptonic and a hadronic tensor,

$$|\mathcal{M}|^2 = L^{\mu\nu} W_{\mu\nu}. \quad (14.7)$$

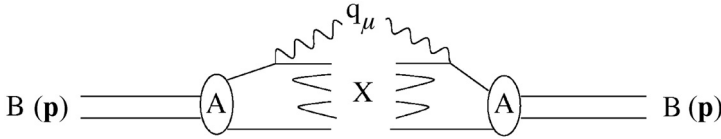


Figure 14.2. Semileptonic B decay in the parton model.

The hadronic tensor can be written as

$$\begin{aligned}
 W_{\mu\nu}(q^2, q \cdot p) &= \frac{1}{2\pi} \int d^4x e^{iqy} \langle B | [J_\mu(x), J_\nu(0)] | B \rangle \\
 &= -g_{\mu\nu} W_1 + p_\mu p_\nu W_2 + i\varepsilon_{\mu\nu\alpha\beta} p^\alpha q^\beta W_3 + \dots, \quad (14.8)
 \end{aligned}$$

with the notation being analogous to that introduced for neutrino reactions. After analyzing the kinematics of the decay, it was shown that a large region of phase space is dominated by the singular behavior of the commutator on the light cone. This allows us to express the decay in terms of a quark distribution function  $f(x)$ , which denotes the probability of finding a b quark in the B meson. Dominance of the light cone demands that the analysis of the decay be carried out in an infinite-momentum frame.

We visualize the B meson moving in an infinite-momentum frame, where the motion of the constituents slows down relative to the time of the decay. In this frame the b quark decays, leaving the rest of the B meson undisturbed. The decay is in general given by

$$\begin{aligned}
 \frac{d\Gamma}{dE_e dq_0 dq^2} &= \frac{G^2 |V_{ub}|^2}{32\pi^3 m_B} \left\{ 2q^2 W_1 + (4E_e q_0 - 4E_e^2 - q^2) W_2 \right. \\
 &\quad \left. - 2q^2 (2E_e - q_0) \frac{W_3}{m_B} \right\}. \quad (14.9)
 \end{aligned}$$

The hadronic tensor for point-like interaction is

$$W_0^{\mu\nu}(q^2, q \cdot p) = \frac{1}{2} \text{Tr}[\not{p}_u \gamma^\mu (1 - \gamma_5) \not{p}_b \gamma^\nu (1 - \gamma_5)] \delta[(p_b - q)^2], \quad (14.10)$$

with  $p_u$  and  $p_b$  the four-momenta of the u and b quarks, respectively. The b quark carries a fraction  $x$  of the B meson's momentum and has the momentum distribution function  $f(x)$ . We arrive at the B-meson decay by substituting

$$p_b = xP \quad \text{and} \quad p_u = p_b - q, \quad (14.11)$$

then multiplying  $W_0^{\mu\nu}$  by  $f(x)$  and integrating over  $x$ ,

$$W^{\mu\nu} = \int W_0^{\mu\nu}(q^2, xq \cdot p) f(x) \delta(x^2 p^2 - 2xq \cdot p + q^2) dx. \quad (14.12)$$

The  $\delta$ -function has two roots  $x_{\pm} = (q_0 \pm |\vec{q}|)/M_B$ . The smaller root  $x_-$  corresponds to diagrams with particles moving backwards in time and will be neglected because it is numerically small. The structure functions are given as (Bareiss and Paschos, 1989)

$$W_1 = 2x_+ f(x_+), \quad W_2 = \frac{4M_B}{|\vec{q}|} x_+^2 f(x_+), \quad W_3 = -\frac{2M_B}{|\vec{q}|} x_+ f(x_+). \quad (14.13)$$

Direct substitution leads to the final result

$$\frac{d\Gamma}{dE_e dq_0 dq^2} = \frac{G^2 |V_{ub}|^2}{4\pi^3 m_B} \frac{x f(x)}{\sqrt{q_0^2 - q^2}} (q_0 - E_e) (2E_e m_B x - q^2), \quad (14.14)$$

with  $x = (q_0 + |\vec{q}|)/M_B$ .

It is hard to measure the triple differential decay and several integrations must be carried out. We define the limits of the integrations. For fixed  $q^2$  we can substitute  $q_0$  by the hadronic mass  $s = m_X^2$ :

$$\begin{aligned} s &= m_B^2 + q^2 - 2m_B q_0, \\ &= m_B^2 + q^2 - 2m_B E_e - 2m_B E_\nu. \end{aligned} \quad (14.15)$$

We can replace  $E_\nu$  by  $E_\nu = q^2/[2E_e(1 - \cos\theta)]$  and obtain the upper bound of  $s$  at  $\cos\theta = -1$ :

$$m_\pi^2 \leq s \leq (m_B - 2E_e) \left( m_B - \frac{q^2}{2E_e} \right). \quad (14.16)$$

The other two variables are bounded in the regions

$$0 \leq q^2 \leq 2m_B E_e, \quad (14.17)$$

$$0 \leq E_e \leq \frac{m_B}{2}. \quad (14.18)$$

The triple differential rate can be used to extract the distribution function directly, but decay rates in several variables are not available yet. Instead one adopts an *Ansatz* for the distribution function. Here we are guided by physical intuition and the experience gained from the fragmentation functions. In the boosted frame, we expect the heavy quark to carry most of the momentum of the meson, which means that the distribution function is peaked at  $x \approx 1$ . Thus a function with a peak in the high- $x$  region and a small width should be sufficient. A function with two parameters  $a$  and  $b$  that satisfies the above criteria is

$$f(x) = N \frac{x(1-x)}{(x-b)^2 + a^2}, \quad (14.19)$$



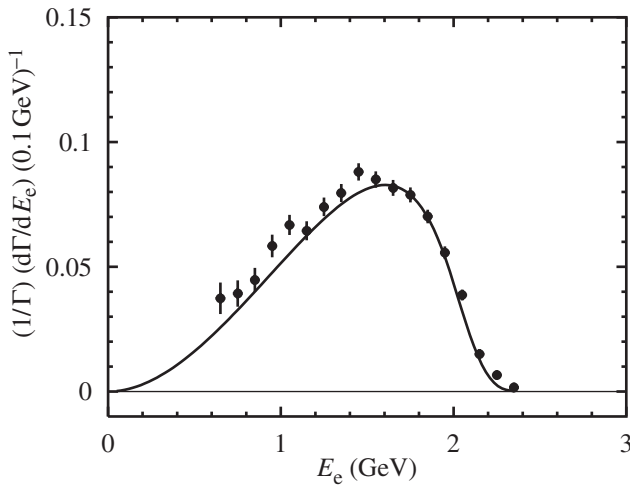


Figure 14.3. The predicted electron-energy spectrum compared with data.

with  $N$  a normalization constant. Integration over the variables and for  $a = 0.0118$ ,  $b = 0.931$  produces the electron spectrum shown in Fig. 14.3. A similar curve is obtained in the ACCMM model. The data points are from Barish *et al.* (1996).

It is desirable to calculate the distribution function or determine its parameters from basic principles. Attempts in this direction have been made in the heavy-quark effective theory.

### 14.3 Exclusive semileptonic decays

Of special interest are decays in which the initial and final mesons are specific hadrons. In this case analysis in the quark-decay picture is not applicable. Let us concentrate on decays of a heavy B or D meson, to a meson  $X_i$  and a lepton pair:

$$M \rightarrow X_i e \nu, \tag{14.20}$$

where  $M$  is the initial heavy meson. The experiments measure the energy spectrum of the electron  $(1/\Gamma)d\Gamma/dE$ , and, for comparison with the theoretical model, we calculate the invariant amplitude for the process. It is again a product of the known leptonic weak current  $L^\mu$  and the hadronic matrix element  $H^\mu$ :

$$\mathcal{M} = \frac{G}{\sqrt{2}} L^\mu H_\mu \quad \text{with} \quad H^\mu = \langle X_i | j^\mu | M \rangle. \tag{14.21}$$

The explicit structure of the meson current depends on the definite properties of the final meson under Lorentz transformations. With such information it is possible

to derive the most general form-factor decomposition of the matrix element. As an example we present here the decay to a pseudoscalar state, i.e.  $X_i = P(0^-)$ :

$$\langle P | j_\mu | M \rangle = \frac{m_M^2 - m_P^2}{q^2} q_\mu F_0(q^2) + \left[ (k_M + k_P)_\mu - \frac{m_M^2 - m_P^2}{q^2} q_\mu \right] F_1(q^2), \quad (14.22)$$

with  $q_\mu = (k_M - k_P)_\mu$  and  $F_0(0) = F_1(0)$ .  $F_0(q^2)$  and  $F_1(q^2)$  denote the longitudinal and transverse form factors, respectively. The form factors are unknown parameters, which have to be estimated theoretically and then compared with the experiments. On the theoretical side, the most famous parametrization appears in the BSW model (Wirbel *et al.*, 1985) which makes the following *Ansatz* for the  $q^2$  dependence:

$$F_i(q^2) = \frac{F_i(0)}{1 - q^2/m_i^2}. \quad (14.23)$$

The pole masses  $m_i$  are estimated numerically. Finally, to predict an energy spectrum for the lepton produced in the decay of Eq. (14.20), an estimate for the form factors at  $q^2 = 0$  is required. In the BSW approach it is given by the overlap of the initial and final wave functions of the mesons. With this information, the phase-space integrals can be performed and many differential decay rates calculated (Wirbel *et al.*, 1985).

#### 14.4 Heavy-quark effective theory

The heavy-quark effective theory (HQET) is a systematic method for describing particles containing a heavy quark (Manohar and Wise, 2000). The HQET is based on the fact that QCD is flavor-blind and a hadron containing a heavy quark is very unlikely to have excitations containing antiquark degrees of freedom. Thus it suffices to work with the spinor of the heavy quark and view the light quark with its surrounding gluonic field as a composite system. This picture is an improvement over the spectator model and supplies a method for calculating the distribution function of the heavy quark in the meson. For mesons made up of a heavy quark  $Q$  and a light antiquark, the heavy quark is essentially on-shell and therefore static when the meson is at rest. This is analogous to atoms, in which the nucleus is stationary and the electrons move in the static field of the nucleus. We will see that, to zeroth order, properties of the meson do not depend on the mass, spin, or flavor of the heavy quark, just as chemical properties of the atom do not depend on the particular isotope.

We shall demonstrate that the HQET is a limiting case of QCD where  $m_Q \rightarrow \infty$  with the four-velocity of  $Q$ ,  $v_\mu$ , held fixed. In this limit the Lagrangian simplifies

considerably, giving a static term and calculable corrections expressed in inverse powers of the heavy-quark mass.

The four-momentum of the heavy quark can be expressed by

$$p_\mu = m_Q v_\mu + k_\mu, \tag{14.24}$$

with  $v_\mu$  its velocity normalized to unity,  $v_\mu v^\mu = 1$ . The correction term  $k_\mu$  is small relative to  $m_Q v_\mu$ . The heavy-quark field has an energy dependence close to that of a free particle and a spinor  $h_v$  with positive energy. Since the heavy quark is bound, it may be influenced by the cloud of quark–antiquark pairs. These degrees of freedom are represented in HQET by two spinors, which are eigenfunctions of the velocity operator. To be specific,

$$Q(x) = e^{-im_Q v \cdot x} [h_v(x) + l_v(x)], \tag{14.25}$$

with

$$\not{v} h_v = h_v, \quad \not{v} l_v = -l_v. \tag{14.26}$$

Factoring out the phase is a redefinition of the field, but the decomposition into the components  $h_v$  and  $l_v$  is an approximation in terms of positive and negative velocity fields.

The results can be re-expressed in terms of velocity projection operators

$$P_\pm = \frac{1}{2}(1 \pm \not{v}), \tag{14.27}$$

which project out the positive velocity fields,

$$P_+ Q = e^{-im_Q v \cdot x} h_v, \tag{14.28}$$

and the negative velocity fields,

$$P_- Q = e^{-im_Q v \cdot x} l_v. \tag{14.29}$$

The overall phase varies rapidly and among the spinors we expect  $h_v$  to be dominant.

The heavy quark interacts with the gluonic field and satisfies a Dirac Lagrangian

$$\mathcal{L} = \bar{Q}(x) [i\not{D} - m_Q] Q(x), \tag{14.30}$$

where  $D_\mu = \partial_\mu + ig_s A_\mu^a \cdot \lambda^a/2$ , with  $A_\mu^a(x)$  the field of the gluons. We are interested in approximate solutions of the Lagrangian in which the heavy-quark field  $h_v$  is slightly perturbed by the light degrees of freedom. To simplify the algebra we mention two identities and drop the subscript  $v$ , i.e. setting  $h_v = h$  and  $l_v = l$ ,

$$\begin{aligned} P_+ \gamma_\mu P_+ &= P_+ (P_- \gamma_\mu + v_\mu) = v_\mu P_+, \\ P_- \gamma_\mu P_- &= P_- (P_+ \gamma_\mu - v_\mu) = -v_\mu P_-, \end{aligned} \tag{14.31}$$

$$\not{D} Q(x) = -im_Q \not{v} Q + e^{-im_Q v \cdot x} (\not{D} h + \not{D} l), \tag{14.32}$$

with  $\bar{h}l = 0$  and  $\bar{h}\not{p}l = \bar{l}\not{p}h = 0$ . With the help of the identities, we rewrite  $\mathcal{L}$  in the following way:

$$\begin{aligned}\mathcal{L} &= \bar{h}i\not{D}h + \bar{l}(i\not{D} - 2m_Q)l + \bar{h}i\not{D}l + \bar{l}i\not{D}h \\ &= i\bar{h}v \cdot Dh - \bar{l}(iv \cdot D + 2m_Q)l + \bar{h}i\not{D}l + \bar{l}i\not{D}h.\end{aligned}\quad (14.33)$$

In the last two terms a final simplification is possible, which allows one to replace  $D_\mu$  by its transverse component  $D_{\perp\mu} = D_\mu - D \cdot v v_\mu$  because  $\bar{h}\not{p}l = \bar{l}\not{p}h = 0$ . Several authors use this additional simplification. The Euler–Lagrange equation for the field gives

$$(iv \cdot D + 2m_Q)l = i\not{D}h \implies l = \frac{1}{iv \cdot D + 2m_Q} i\not{D}h. \quad (14.34)$$

To sum up, we have taken out the dependence on large momenta by factoring out the term  $\exp(-im_Q v \cdot x)$ . The remaining terms, except for the covariant derivative acting on  $h$ , contain small momenta, as is evident from the fact that  $l(x)$  is indeed the smaller of the two velocity spinors.

In this limit of the theory, we give rules for the propagator

$$i\frac{\not{p} + m_Q}{p^2 - m_Q^2} = i\frac{m_Q\not{v} + m_Q + \not{k}}{2m_Q v \cdot k + k^2} \rightarrow \frac{i}{v \cdot k} \left( \frac{1 + \not{v}}{2} \right) + \mathcal{O}\left(\frac{k}{m_Q}\right) \quad (14.35)$$

and for the vertex describing the coupling of gluons to the heavy quark,

$$ig\bar{h}\gamma_\mu h = igv_\mu \bar{h}h. \quad (14.36)$$

Calculations with  $h$  alone reproduce the free-quark model. The interactions are improved by including  $1/m_Q$  terms.

In the limit of  $m_Q \rightarrow \infty$  the quark field approaches the heavy-quark field,

$$Q(x) \rightarrow e^{-im_Q v \cdot x} P_+ h. \quad (14.37)$$

On substituting this field into the Lagrangian (14.30) or from Eq. (14.33), we obtain

$$\mathcal{L} \rightarrow i\bar{h}v \cdot Dh = \mathcal{L}_0. \quad (14.38)$$

The result shows explicitly that in the limit  $m_Q \rightarrow \infty$  the interaction between the gluonic field and the heavy quark is independent of the spin and mass of the heavy quark. There are several consequences of this property.

As mentioned already, the meson is viewed as composed of a heavy quark and a light system consisting of the light quark and its surrounding gluonic field. Several properties should be independent of the spin of the heavy quark. Let us denote the

spin of the light system by  $S_\ell$  and the spin of the heavy quark by  $S_Q = \frac{1}{2}$ . The two systems may still have relative angular momentum  $\vec{L}$ . The total angular momentum,  $\vec{J}$ , for the meson is a sum of spins

$$\vec{S} = \vec{S}_Q + \vec{S}_\ell \tag{14.39}$$

plus the relative angular momentum  $\vec{L}$ ,

$$\vec{J} = \vec{S} + \vec{L}.$$

For a meson with  $S_\ell = \frac{1}{2}$  and  $\vec{L} = 0$

$$|\vec{S}| = |\vec{S}_\ell| \pm \frac{1}{2} = 0, 1$$

and the total angular momentum  $\vec{J} = 0$  or  $1$ . For  $Q = b$  the two states with  $L = 0$  are  $B_d$  and  $B_d^*$  mesons. The HQET predicts that the two states have properties that are independent of  $S_Q$  and therefore degenerate. The difference between the masses of the pseudoscalar and vector mesons is indeed small relative to their sum. The same is experimentally true for the charm states  $D$  and  $D^*$ .

Even though the mass differences are small, they are not zero, suggesting that we must formulate the effective Lagrangian more precisely by keeping the  $1/m_Q$  terms which were ignored. This will be discussed in the next section. The same is true for the charm states  $D$  and  $D^*$  containing charm quarks. To first approximation the spin symmetry is realized. However, the small differences suggest that we must formulate the effective Lagrangian more accurately by including  $1/m_Q$  corrections.

### 14.5 The effective Lagrangian: $1/m_Q$ corrections

Higher-order corrections are obtained by including the light-quark degrees of freedom. This complicates the algebra somewhat, but leads to correction terms that are simple to describe. In the following we give a derivation. However, the reader who finds it complicated may proceed directly to Eq. (14.43).

To include the light-quark field, we substitute  $l(x)$  using Eq. (14.34) together with a similar expression for  $\bar{l}(x)$ . In this way we obtain an improved interaction,

$$\begin{aligned} \mathcal{L} = \mathcal{L}_0 + \mathcal{L}_1 &= \bar{h} \left( i \not{D} + i \not{D} \frac{1}{i v \cdot D + 2m_Q} i \not{D} \right) h + \mathcal{O} \left( \frac{1}{m_Q^2} \right) \\ &= i \bar{h} v \cdot D h + \frac{1}{2m_Q} \bar{h} i \not{D} i \not{D} h + \mathcal{O} \left( \frac{1}{m_Q^2} \right), \end{aligned} \tag{14.40}$$

with the first term being  $\mathcal{L}_0$  and the rest the improvement. The new term has two covariant derivatives next to each other and can be simplified. We use the identity

$$\begin{aligned} \not{D}\not{D} &= \gamma^\mu \gamma^\nu D_\mu D_\nu \\ &= \frac{1}{2} \{\gamma^\mu, \gamma^\nu\} D_\mu D_\nu + \frac{1}{2} [\gamma^\mu, \gamma^\nu] D_\mu D_\nu \\ &= D^2 + \frac{1}{4} [\gamma^\mu, \gamma^\nu] [D_\mu, D_\nu] \end{aligned} \quad (14.41)$$

together with

$$\sigma^{\mu\nu} = \frac{i}{2} [\gamma^\mu, \gamma^\nu], \quad i g_s G_{\mu\nu}^a \left( \frac{\lambda_a}{2} \right) = [D_\mu, D_\nu], \quad (14.42)$$

in order to obtain the  $1/m_Q$  term of the Lagrangian:

$$\mathcal{L}_1 = -\bar{h} \frac{D^2}{2m_Q} h - g_s \bar{h} \frac{\sigma^{\mu\nu} G_{\mu\nu}}{4m_Q} h. \quad (14.43)$$

A few remarks are now in order. The first term,  $D^2/(2m_Q)$ , is the average kinetic energy of the heavy quark. The second term couples the spin of the heavy quark to the gluo-magnetic field surrounding the quarks. The theory succeeded in including the interaction of the heavy quark with the surrounding degrees of freedom. It also has the advantage that it is precise enough to allow systematic studies. It has been successful in accounting for mass differences, decay rates etc., which we cover in the next section.

### 14.5.1 Applications

#### Mass relations

To leading order the HQET Lagrangian does not depend on the spin or flavor of the heavy quark. The first term in Eq. (14.43) breaks the flavor symmetry and the second term breaks both flavor and spin symmetries. These two terms play a leading role in determining the mass spectra of heavy hadrons. Consider the expectation value of the Hamiltonian between mesonic states. The mass of the meson is written as

$$\begin{aligned} m_M &= m_Q + \bar{\Lambda} + \langle M | O_1 | M \rangle + \langle M | O_2 | M \rangle \\ &= m_Q + \bar{\Lambda} - \frac{\lambda_1}{2m_Q} + \frac{a_J \lambda_2}{2m_Q}, \end{aligned} \quad (14.44)$$

with  $a_J = \frac{1}{2} \vec{S}_Q \cdot \vec{S}_\ell$ . Here  $O_1$  and  $O_2$  are the first and second operators in Eq. (14.43), respectively, and  $\bar{\Lambda}$  is the contribution from the light-quark degrees of

freedom, which is a priori unknown. According to HQET,  $\lambda_1$  and  $\lambda_2$  are universal constants. One generally determines them from the moments of the energy spectrum of inclusive semileptonic B decays. It turns out that  $\bar{\Lambda} \approx 0.40 \text{ GeV}$  and  $\lambda_1 \approx -0.2 \text{ GeV}^2$ .

$O_2$  is a magnetic-moment-type interaction, and its matrix element for mesons with  $L = 0$  is proportional to  $S_Q \cdot S_\ell = (J^2 - S_Q^2 - S_\ell^2)/2$ . The expectation values of this operator in triplet and singlet states are different, which causes a splitting among the lowest-lying states. The singlet ( $J = 0$ ) is lowered and the triplet ( $J = 1$ ) is raised, but by different amounts. These states are generally denoted by  $M$  and  $M^*$ . It is obvious that

$$\frac{m_{B^*} - m_B}{m_{D^*} - m_D} = \frac{m_c}{m_b},$$

which is satisfied to a high degree of accuracy. In fact, one can determine  $\lambda_2$  from the splitting of the meson doublet.

*Exclusive semileptonic decays*

An important prediction of HQET describes decays governed by the quark-level transition  $b \rightarrow c$ . The initial B meson decays into an electron–neutrino pair plus the D meson. In general the matrix element of pseudoscalar-to-pseudoscalar transition involves two form factors that are functions of  $q^2$  (see Eq. (14.22)). The velocities for the B and D mesons are  $v^\mu = p^\mu/m_B$  and  $v'^\mu = p'^\mu/m_D$  and the  $q^2$  dependence may be replaced by

$$w = v \cdot v' = \frac{m_B^2 + m_D^2 - q^2}{2m_B m_D}. \tag{14.45}$$

In the limit that the masses are very big relative to the difference  $m_B - m_D$  the two states B and D are, according to HQET, very similar. In this limit  $v \cdot v' = 1$  and  $v^\mu \approx v'^\mu$ .

To appreciate the situation, consider a configuration in which the B meson is at rest and the four-momentum carried away by the lepton pair is maximal,  $q^2 = (M_B - M_D)^2$ , which means that the D meson is also produced at rest. This is the zero-recoil point where  $w = 1$ . In the limit that the heavy-meson masses are large and close to each other, only one form factor contributes:

$$\begin{aligned} \langle D(p') | V_\mu | B(p) \rangle &= f_+(q^2)(p + p')_\mu + f_-(q^2)(p - p')_\mu \\ \rightarrow \langle D(v') | \bar{c} \gamma_\mu b | B(v) \rangle &\approx \sqrt{m_B m_D} h(v \cdot v')(v_\mu + v'_\mu). \end{aligned} \tag{14.46}$$

The square root arises from the normalization of the states and  $h(v \cdot v')$  is a universal function called the Isgur–Wise function (Isgur and Wise, 1989, 1990). Furthermore,

in the limit  $m_B, m_D \rightarrow \infty$  with  $m_B - m_D$  fixed,  $q^2 \ll M_B, M_D$ , the Isgur–Wise function measures the overlap of two identical wave functions so that  $h(1) = 1$ .

Consider next the decay to a vector meson  $B \rightarrow D^* \ell \nu$ . We have discussed already the fact that to leading order the decay is independent of the spin of the heavy quarks. A consequence of the symmetry is the relation

$$\langle D^*(v', \varepsilon) | \bar{c} \gamma_\mu b | B(v) \rangle = i \sqrt{m_B m_{D^*}} \epsilon_{\mu\nu\alpha\beta} \epsilon^\nu v^\alpha v'^\beta h(v \cdot v'), \quad (14.47)$$

where the Lorentz structure depends on the polarization of the  $D^*$  meson,  $\epsilon^\mu$ , and the same universal form factor  $h(v \cdot v')$  appears as before. However, the universality is a feature of the zeroth-order Lagrangian and is broken by  $1/m_Q$  corrections. For a complete analysis we must also include matrix elements of the axial current, which bring additional form factors into play. The general case must explain decays to several vector mesons  $D^*(2010)$ ,  $D^*(2420)$ ,  $\dots$ , whose partial decay widths are different from each other. The differences remain after corrections over phase-space factors have been taken into account.

This motivated an analysis of the partial decay rates in terms of  $h(v \cdot v')$  plus its slope at the point  $v \cdot v' = 1$ . The important variable for the decays is  $w$ , with the decay spectrum given by (Manohar and Wise, 2000)

$$\frac{d\Gamma}{dw}(B \rightarrow D^* \ell \nu) = \frac{G^2 |V_{cb}|^2}{48\pi^3} K(w) h(v \cdot v')^2, \quad (14.48)$$

where  $w$  is defined in (14.45),  $K(w)$  is a known phase-space factor, and  $h(v \cdot v')$  is the Isgur–Wise function including finite-mass and other (QCD,  $\dots$ ) corrections. The analysis determined the value of the form factor  $F_1(w = 1)$  and its slope at  $w = 1$ . A systematic analysis of several experiments gives the mean value of the slope and the product as

$$h(w = 1) |V_{cb}| = 0.0038 \pm 0.0010,$$

from which the value for  $|V_{cb}|$  has been extracted (see Section 9.3.4).

The applications of HQET to mass relations and B decays to D and  $D^*$  are successes of the theory. The Isgur–Wise function  $h(v \cdot v')$  has been studied and calculated also in lattice gauge theories. Of direct interest is its calculation for the physical b and c masses in the zero-recoil limit (when  $v \cdot v' = 1$ ). Lattice calculations give  $h(1) = 0.929$  with a small error.

B-meson decays to light mesons are much harder to calculate in HQET or on the lattice because most of the decay occurs in a kinematic region where the  $\pi$  or the  $\rho$  mesons have large momenta. They attract a good deal of attention because data



on B-meson decays are accumulating in B-factories and are very important for the interpretation of CP asymmetries in B-meson decays.

#### *Inclusive semileptonic decays*

For inclusive decays one must calculate the decay rate in the rest frame of the b quark. To leading order the hadronic tensor will have the structure of Eq. (14.10), which is proportional to the  $\delta$ -function

$$\delta[(p_b - q)^2] = \delta(m_b^2 - 2p_b \cdot q + q^2).$$

In the limit  $m_b^2 \gg q^2$  it reduces to

$$\delta(m_b^2 - 2m_b q_0),$$

which peaks at the endpoint of the  $q_0$  range. Since there is no averaging over a distribution function, the smoothness of the spectrum must be brought about by higher-order corrections of HQET. Higher-order corrections including bound-state effects must reproduce the effects and spectrum discussed in Sections 14.2.1 and 14.2.2.

### **14.6 The top quark and its physical properties**

The top quark is very heavy and weighs as much as a heavy atom. After the discovery of the bottom quark and the tau lepton, the top was predicted in order to preserve the symmetry between quarks and leptons. In addition, several properties of the low-lying states required the existence of a heavier state. Among these properties are the mixing and CP properties of the neutral K mesons, as well as those of neutral D and B mesons. Furthermore, in order to accommodate CP violation in the electroweak theory, a third generation of quarks is required. Some of these properties were mentioned earlier and they will be covered in greater detail in the next chapters.

Besides the expectation of a heavier top quark, its mass was, for a long time, unknown. Only with the discovery of the W and Z bosons and the precise measurements of their masses and widths did it become possible to put a limit on the top quark's mass. A stringent limit is provided by the  $\rho$  parameter, where the correction from the self-energy has a quadratic dependence on the quark mass. We quote the result here in order to stress how quantum corrections become important. The  $\rho$  parameter is defined as

$$\rho = \frac{M_W^2}{M_Z^2 \cos^2 \theta_W}$$

and has the value unity (see Eq. (12.19)). The loop correction from the top–bottom quark pair changes this ratio to

$$\rho = 1 + \frac{G}{8\pi^2} \left( m_t^2 + m_b^2 - \frac{2m_t^2 m_b^2}{m_t^2 - m_b^2} \ln \left( \frac{m_t^2}{m_b^2} \right) + \text{smaller terms from Higgs exchanges} \right). \quad (14.49)$$

For very accurate values of  $M_W$ ,  $M_Z$ , and the mixing angle, the effect from the top quark is noticeable. Several analyses along these lines gave a range for the top quark's mass in the neighborhood of 175 GeV, with an error of  $\pm 25$  GeV, within which it was eventually discovered.

The dominant decay of the top quark is into a bottom quark plus a W boson. The calculation of the decay is straightforward and we have formulated it as an exercise. If we neglect the mass of the bottom quark, the decay width is

$$\Gamma(t \rightarrow bW^+) = \frac{G_F M_t^3}{8\sqrt{2}\pi} |V_{tb}|^2 \left( 1 - \frac{M_W^4}{M_t^4} \right)^2, \quad (14.50)$$

which grows rapidly with the top-quark mass. For  $M_t = 175$  GeV, the decay width is

$$\Gamma(t \rightarrow bW^+) = 1.55 \text{ GeV},$$

which corresponds to a top-quark lifetime of  $0.4 \times 10^{-24}$  s. The confining effects of the strong interactions act on a time scale  $\approx 1/\Lambda_{\text{QCD}}$ . This means that the top quark decays long before the interaction can act to produce hadrons. Unlike the properties of the other five quarks, there are no bound states and no toponium spectroscopy.

The fact that the mass of the top quark is close to the value required by the radiative corrections is a success of the electroweak theory. These and other tests of the theory will be discussed in Section 17.2 devoted to precision tests of the theory. Another test involves the value of  $V_{tb}$ , which, according to the analysis of the CKM matrix, must be very close to unity. There is already experimental evidence that the top decays primarily to a bottom quark, but the accuracy is still very poor to test the unitarity prediction in Eq. (9.49).

The ultrarapid decay of the top quark implies that the production of  $t\bar{t}$  pairs in hadron collisions should be calculable in perturbative QCD. Electron–positron colliders could be used to search for the reaction

$$e^+e^- \rightarrow t\bar{t},$$

but at the lower energies available in those colliders it is impossible to produce the pairs. The decisive experiments have been carried out at the proton–antiproton

collider of Fermilab. Some characteristic reactions and their decays are listed below:

$$\begin{aligned}
 p + \bar{p} &\rightarrow t + \bar{t} + \text{anything} \rightarrow e\nu_e + \mu\bar{\nu}_\mu + \text{hadrons}, \\
 &\rightarrow e^\pm\mu^\pm b\bar{b} \cancel{E}_T, \\
 &\rightarrow \mu^\pm + \text{jets } \cancel{E}_T.
 \end{aligned}$$

The dilepton events ( $e\mu$ ,  $ee$ , and  $\mu\mu$ ) are produced when both  $W$  bosons decay into  $e\nu$  or  $\mu\nu$ . The neutrinos remain unobservable and are represented by the missing energy  $\cancel{E}_T$ . Events with lepton-plus-jets channels occur when one  $W$  decay produces  $e$  or  $\mu$  and the other decays into quark–antiquark pairs.

A second challenge to experimenters is the complexity of the events in high-energy proton–antiproton collisions. The  $t\bar{t}$  pair produced is accompanied by scores of other particles. Separating the top quark is like searching for a needle in a haystack. Two experimental groups at the Tevatron collider at Fermilab succeeded in discovering the production of  $t\bar{t}$  pairs. As mentioned in the introduction to this chapter, the production of  $t\bar{t}$  pairs and their subsequent decays are computed in the parton model, using the best possible quark distribution functions, and the top quark’s mass is determined as the value which optimizes the fit.

We close this section with a speculation. The fact that the mass of the top quark is larger than the mass of gauge bosons and closer to the scale of the symmetry-breaking motivates the thought that the top quark is intimately connected to the symmetry-breaking. One suggestion is to study the decays of the top quark to the  $b$  quark and the  $W$  boson, which is expected to be longitudinally polarized. Since the longitudinal state of  $W$  bosons is developed through the Higgs mechanism, it may be sensitive to new physics. In another suggestion, the top–antitop pairs attract each other through a new force to make a condensate, which is the Higgs particle. We return to this possibility in Chapter 17.

## 14.7 Loop diagrams with heavy quarks

### 14.7.1 Mixing of states and lifetime differences: a preview

Heavy quarks also appear as intermediate states in loop diagrams and give dominant contributions. As a first example we study box diagrams, in which second-order weak interactions change the flavor quantum number by two units and produce the mixing of  $B^0$ – $\bar{B}^0$ , as well as  $K^0$ – $\bar{K}^0$ , states. When the intermediate states are heavy quarks, they produce a short-distance interaction shown with the diagrams in Fig. 14.4. The strategy of the calculations is to construct an effective  $\Delta F = 2$  Lagrangian from the free-quark model and then take the matrix element between  $B^0$  and  $\bar{B}^0$  (or, analogously,  $K^0$  and  $\bar{K}^0$ ). We compute the diagram of Fig. 14.4 in

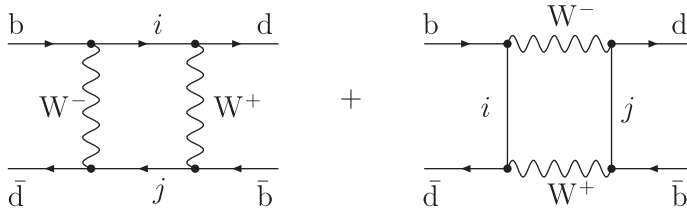


Figure 14.4. Box diagrams for  $\Delta B = 2$  transitions. We calculate the “scattering” term in (a). The “annihilation” term (b) is equal to the “scattering” term.

Section 14.7.2, where it is also shown that box diagrams are finite, i.e. they do not bring in any ultraviolet divergences. Before we present the calculation, we quote several results from Chapters 15 and 16 in order to emphasize the point that box diagrams are indeed important. The interested reader may consult Chapters 15 and 16 for the underlying physics and then return to this section for the study of a loop diagram.

Let us denote by  $\Delta M_d = M_{B_H} - M_{B_L}$  the difference in mass between the physical states built up from the mesons  $B_d^0$  and  $\bar{B}_d^0$ . We use the subscripts H and L to denote heavy and light mesonic states. The structure of physical states is described in Chapter 15. The calculation of the box diagram with the top quark in the intermediate state gives

$$\Delta M_d = \frac{G^2}{16\pi^2} |V_{td} V_{tb}^*|^2 M_W^2 E(x_t) X_{B_d}, \quad \text{with} \quad x_t = \left( \frac{m_t}{m_W} \right)^2, \quad (14.51)$$

$$E(x_t) = \frac{3}{2} \frac{x_t^3}{(1-x_t)^3} \ln x_t - \left[ \frac{1}{4} + \frac{9}{4} \frac{1}{1-x_t} - \frac{3}{2} \frac{1}{(1-x_t)^2} \right] x_t, \quad (14.52)$$

$$\bar{X}_{B_d} = \langle B_d | \bar{d} \gamma_\mu (1 - \gamma_5) b \bar{b} \gamma^\mu (1 - \gamma_5) d | \bar{B}_d \rangle. \quad (14.53)$$

The function  $E(x_t)$  comes from the integration over the loop and  $X_{B_d}$  is the matrix element of a four-quark operator between  $B_d$  and  $\bar{B}_d$  states. Four-quark operators appear as overall factors in calculations of box diagrams. The same calculation also determines the width difference

$$\Delta \Gamma_d = \frac{3G^2}{32\pi} m_b^2 |V_{td} V_{tb}^*|^2 X_{B_d}. \quad (14.54)$$

In the decay only u and c quarks appear as final states. The decay is discussed at the end of Section 16.4 and shown in Fig. 16.1. The dependences of the width and  $\Delta M_d$  on the quark masses are different. Mass and width differences are related by

$$\Delta \Gamma_d = \frac{3}{2} \pi \frac{m_b^2}{M_W^2 E(x_t)} \Delta M_d, \quad (14.55)$$

from which we conclude that for large  $m_t$  the width difference is much smaller than the mass difference. Furthermore, on comparing  $\Delta M_d$  with the decay width

$$\Gamma_B = \frac{G^2 m_b^5}{192\pi^3} |V_{bc}|^2, \quad (14.56)$$

we note that there is an enhancement of the mass difference arising from the high mass of the heavy quark. Thus, for favorable values of the other quantities,  $\Delta M_d$  can be comparable to  $\Gamma_B$ . In fact, experiments determined

$$\Delta M_d = (0.49 \pm 0.01) \times 10^{12} \hbar s^{-1}, \quad (14.57)$$

which is one fifth of the width. A similar analysis of the mass difference of  $B_s = (b\bar{s})$  leads to a larger mass difference because it is enhanced by the CKM element. Experimentally there is the lower bound

$$\Delta M_s > 13.1 \times 10^{12} \hbar s^{-1}. \quad (14.58)$$

The discussion shows that loop contributions are important since they determine physical quantities and correlate properties of various mesons.

The physics described for the neutral  $B_d$  mesons contains several general properties. The down quarks are always lighter than the upper quark of the same family. Consequently, mesons containing down quarks decay to quarks of a lighter family, for which the decay width is suppressed by a CKM element. On the other hand, the mass difference of neutral mesons containing the down quarks involves the square of the mass of the upper quark. If the mass of the upper quark in the same family is much larger and the values of the mixing angles and the reduced matrix element are favorable, then substantial mixing between the neutral mesons is possible. This situation is realized for the  $B_d^0$ ,  $B_s^0$ , and  $K_L^0$ - $K_S^0$  mesons.

The opposite situation prevails for neutral mesons that contain a heavy upper quark. For example, for  $D^0 = (c\bar{u})$  mesons the decay width is proportional to  $m_c^5$  and the CKM element is practically unity. The mass difference is proportional to  $m_b^2$  or  $m_s^2$  and the CKM elements are smaller than unity, so there is no substantial enhancement. Consequently, mixing of the  $D^0$  and  $\bar{D}^0$  states is small and it has not been observed yet.

### 14.7.2 Calculation of a box diagram

We compute first the box diagrams for Fig. 14.4 with intermediate quarks  $i, j = u, c, t$ . In addition to the diagrams with the exchange of W bosons there are exchanges with charged Higgses, which become important when the masses of the internal quarks are large. Charged Higgses became the longitudinal degrees of freedom of the W bosons. For simplicity we shall assume that the external momenta

and masses are zero. In the Feynman–'t Hooft gauge, we obtain

$$\begin{aligned}
 T_{12}^a &= \left(\frac{g}{2\sqrt{2}}\right)^4 \sum_{i,j} \lambda_i \lambda_j \int \frac{d^4k}{(2\pi)^4} \left(\frac{-i}{k^2 - M_W^2}\right)^2 \left(\bar{d}_L \gamma^\mu \frac{\not{k} + m_i}{k^2 - m_i^2} \gamma^\nu b_L\right) \\
 &\quad \times \left(\bar{d}_L \gamma_\nu \frac{\not{k} + m_j}{k^2 - m_j^2} \gamma_\mu b_L\right) \\
 &= -\frac{g^4}{64} \sum_{i,j} \lambda_i \lambda_j \int \frac{d^4k}{(2\pi)^4} \frac{1}{(k^2 - M_W^2)^2} \bar{d} \gamma^\mu (1 - \gamma_5) \frac{\not{k} + m_i}{k^2 - m_i^2} \gamma^\nu (1 - \gamma_5) b \\
 &\quad \times \bar{d} \gamma_\nu (1 - \gamma_5) \frac{\not{k} + m_j}{k^2 - m_j^2} \gamma_\mu (1 - \gamma_5) b, \tag{14.59}
 \end{aligned}$$

with  $\lambda_i = V_{id}^* V_{is}$ . Simple counting of the momenta shows that the integral is convergent. The neutrino masses in the numerators do not contribute, because of the  $(1 - \gamma_5)$  structure. The surviving integral has the following Lorentz structure:

$$I_{\alpha\beta}(i, j) = \int d^4k \frac{k_\alpha k_\beta}{(k^2 - M_W^2)^2 (k^2 - m_i^2)(k^2 - m_j^2)} = I(m_i, m_j, M_W) g_{\alpha\beta}. \tag{14.60}$$

The fact that the integral is proportional to the  $g_{\alpha\beta}$  simplifies the spinor structure, which takes the form

$$\bar{d} \gamma^\mu \gamma^\alpha \gamma^\nu (1 - \gamma_5) b \cdot \bar{d} \gamma_\nu \gamma_\alpha \gamma_\mu (1 - \gamma_5) b = 4 \bar{d} \gamma^\alpha (1 - \gamma_5) b \cdot \bar{d} \gamma_\alpha (1 - \gamma_5) b. \tag{14.61}$$

This and other spinor identities follow from the relation

$$\gamma^\mu \gamma^\lambda \gamma^\nu = g^{\mu\lambda} \gamma^\nu + g^{\lambda\nu} \gamma^\mu - g^{\mu\nu} \gamma^\lambda - i \varepsilon^{\mu\lambda\nu\rho} \gamma_5 \gamma_\rho, \tag{14.62}$$

as demonstrated in Appendix C.

### 14.7.3 Integrals in Euclidean space

In the calculation of the integrals we consider the momenta to be Euclidean, by setting

$$k_0 = ik_4. \tag{14.63}$$

Then the propagators do not have poles. The four-dimensional volume element becomes

$$d^4k = dk_0 d^3k = idk_4 d^3k. \tag{14.64}$$

A typical integral in loop calculations takes the form

$$I^\alpha(m) = \int d^4k \frac{1}{(k^2 - m^2 + i\epsilon)^\alpha} = i(-1)^\alpha \int_{\text{Eucl.}} d^4k \frac{1}{(k^2 + m^2 - i\epsilon)^\alpha}. \quad (14.65)$$

In Euclidean space we can transform to spherical coordinates,

$$d^4k \rightarrow k^{4-1} dk d\Omega_4 \quad \text{with} \quad \int d\Omega_4 = \frac{2\pi^2}{\Gamma(2)} = 2\pi^2. \quad (14.66)$$

For our specific integral

$$\begin{aligned} I(m_i, m_j, M_W) &= \frac{1}{4} \int d^4k \frac{k^2}{(k^2 - M_W^2)^2 (k^2 - m_i^2)(k^2 - m_j^2)} \\ &= \frac{1}{4} 2\pi^2 \int_0^\infty dk \frac{k^5}{(k^2 + M_W^2)^2 (k^2 + m_i^2)(k^2 + m_j^2)}. \end{aligned} \quad (14.67)$$

### 14.7.4 Feynman parameters

The standard way of carrying out momentum integrations in loop integrals is to use the so-called Feynman-parameter technique in order to transform a product of propagators depending on the integration momentum into a single factor. This is accomplished with the following identity:

$$\begin{aligned} \frac{1}{(a_1 + i\epsilon)(a_2 + i\epsilon) \dots (a_n + i\epsilon)} &= \int_0^1 (n-1)! dx_1 dx_2 \dots dx_n \\ &\times \frac{\delta(1 - x_1 - x_2 - \dots - x_n)}{[a_1x_1 + a_2x_2 + \dots + a_nx_n + i\epsilon]^n}. \end{aligned} \quad (14.68)$$

Simple examples can be worked out. When the propagator  $(a_i + i\epsilon)^k$ , with  $k$  an integer, appears on the left-hand side, the corresponding formula is obtained by differentiating the above expression with respect to  $a_i$  several times. Following this rule we obtain

$$\frac{1}{(a_1 + i\epsilon)(a_2 + i\epsilon)(a_3 + i\epsilon)} = 6 \int \frac{dx dy (1 - x - y)}{[a_1(1 - x - y) + a_2x + a_3y + i\epsilon]^4}. \quad (14.69)$$

Returning to our integral in Eq. (14.67),

$$\begin{aligned} I(m_i, m_j, M_W) &= \frac{\pi^2}{2} \int_{k=0}^\infty dk k^5 \int_0^1 dx \int_0^{1-x} dy \\ &\times \frac{1 - x - y}{[k^2 + M_W^2(1 - x - y) + m_i^2x + m_j^2y]^4}. \end{aligned} \quad (14.70)$$

Now, since the Feynman parameters in the  $\delta$ -function sum up to unity, the coefficient of the  $k^2$  term in the denominator is always unity. We can perform the  $dk^2$  integration to obtain

$$\begin{aligned}
 I(m_i, m_j, M_W) &= \frac{\pi^2}{12M_W^2} \int_0^1 dx \int_0^{1-x} dy \frac{1-x-y}{(1-x-y+x_i^2x+x_j^2y)} \\
 &= \frac{\pi^2}{12M_W^2} \frac{1}{2} \frac{1}{x_i - x_j} \left[ \frac{1}{1-x_i} - \frac{1}{1-x_j} + \frac{x_i^2}{(1-x_i)^2 \ln x_i} \right. \\
 &\quad \left. - \frac{x_j^2}{(1-x_j)^2 \ln x_j} \right], \quad (14.71)
 \end{aligned}$$

with  $x_i = m_i^2/M_W^2$  and  $x_j = m_j^2/M_W^2$ . This diagram gives the dominant contribution for cases in which  $x_i$  and  $x_j \ll 1$ . In the other cases with the exchange of a heavy scalar, additional diagrams must be included; the complete answer is given in Chapter 15.

This first example shows that the calculation of loop diagrams involves four steps.

1. A simplification of the spin structure, which reduces the calculation to a few four-dimensional integrals.
2. The reduction of the denominators to a single factor with the help of Feynman parameters.
3. The completion of the four-dimensional integrals. This is carried through in Euclidean space and holds in the Minkowskian region by analytic continuation. The case of the box diagram is relatively simple, because the integral is convergent. In the general case, the integrals are divergent, which demanded the development of special methods for subtracting the infinities, which respect the gauge invariance of the theory.
4. Finally, there is an integration over the Feynman parameters, which requires special attention at the endpoints, where infrared singularities may occur.

### Problems for Chapter 14

1. Draw the graph of  $d\Gamma^0/dx$ , where  $x = 2E/W$ , in the quark rest frame. Multiply by the QCD correction factor

$$G(x) = \frac{1}{x} 2 \ln(1-x)[2 + \ln(1-x)]$$

and show how the distribution changes.

2. Use the identities given in the text to prove Eq. (14.33). Then show that it is possible to replace  $D_\mu$  by  $D_{\perp\mu} = D_\mu - D \cdot vv_\mu$ .
3. For the semileptonic decay  $B \rightarrow D e \bar{\nu}$  the dominant form factor  $f_+(q^2)$  is related to the Isgur–Wise function as in Eq. (14.46).



(i) Show that  $f_+(q^2)$  is related to  $h(v \cdot v')$  as follows:

$$f_+(q^2) = h(v \cdot v') \frac{2\sqrt{m_B m_D}}{m_B + m_D}.$$

(ii) Calculate the decay spectrum  $d\Gamma/dW$  in the heavy-quark limit.

(Hint: you may begin with  $d\Gamma/dq^2$  and then take the heavy-quark limit.)

4. Use the Feynman rules from Chapter 8 to calculate the decay width for the top quark given in Eq. (14.50).
5. Prove the following useful identities that involve Feynman parameters:

$$(i) \quad \frac{1}{(a_1 + i\varepsilon)(a_2 + i\varepsilon)} = \int_0^1 \frac{dx}{[a_1 x + a_2(1-x) + i\varepsilon]^2};$$

$$(ii) \quad \frac{1}{(a_1 + i\varepsilon)^3(a_1 + i\varepsilon)} = \int_0^1 \frac{3x^2 dx}{[ax + b(1-x) + i\varepsilon]^4}.$$

### References

- Altarelli, G., Cabibbo, N., Gorbo, G., Maiani, L., and Martinelli, G. (1982), *Nucl. Phys.* **B208**, 365
- Bander, M., Silverman, D., and Soni, A. (1980), *Phys. Rev. Lett.* **44**, 7–9  
(for another explanation, see M. Lusignoli and A. Pugliese, hep-ph/0210071)
- Bareiss, A., and Paschos, E. A. (1989), *Nucl. Phys.* **B327**, 353
- Barish, B., Chandra, M., Chan, S. *et al.* (1996), *Phys. Rev. Lett.* **76**, 1570
- Combination of CDF and DO Results on Top Quark Mass (CDF/DO), hep-ex/0507006
- Glashow, S. L., Iliopoulos, J., and Maiani, L. (1970), *Phys. Rev.* **D2**, 1285
- Isgur, N., and Wise, M. (1989), *Phys. Lett.* **B232**, 113  
(1990), *Phys. Lett.* **B237**, 527
- Manohar, A. (2000), *Eur. Phys. J.* **C15**, 377–380
- Manohar, A. V., and Wise, M. B. (2000), *Heavy Quark Physics* (Cambridge, Cambridge University Press)
- Narison, S. (2001), *Phys. Lett.* **B520**, 115; hep-ph/0108065
- The CDF collaboration, the DO collaboration and the Tevatron Electroweak Working Group
- Wirbel, M., Stech, B., and Bauer, M. (1985), *Z. Phys.* **C29**, 637

### Select bibliography

Many topics of heavy-quark theory are presented in the book

Manohar, A. V., and Wise, M. (2000), *Heavy Quark Physics* (Cambridge, Cambridge University Press)

For an overview of top-quark physics, see

Quigg, C. (1997), *Phys. Today*, May, p. 20